Sensing-Throughput Tradeoff for Cognitive Radio as Interweave Systems: A Deployment-Centric Viewpoint

Ankit Kaushik*, Shree Krishna Sharma†, Symeon Chatzinotas†,
Björn Ottersten†, Friedrich K. Jondral*

Abstract

Cognitive Radio is envisaged as one of potential candidate that addresses the issue of spectrum scarcity. Secondary access to the licensed spectrum is viable only if the interference is avoided at the primary system. In this regard, different paradigms have been conceptualized. Of these, Interweave Systems (ISs) that employ spectrum sensing have been widely investigated in the literature. This makes performance characterization of a cognitive radio system critical, hence, an interesting research problem. Baseline models investigated in the literature characterize the performance of IS in terms of sensing-throughput tradeoff assumes, however, channels' knowledge at secondary transmitter. In practice, this knowledge is unavailable. As a result, these models depicts an ideal scenario, thereby leaving the performance characterization based on these models disputable and impractical for hardware deployment. Motivated by this fact, we establish a novel model that incorporates channel estimation in the system. Based on the proposed model, this work investigates the impact of estimation on the performance of IS. More particularly, the distortion induced in the probability of detection affects the performance of the detector, that may result in severe interference at the primary users. To capture this effect, we propose two new primary user constraints namely, average and outage constraints on the probability of detection. Our analysis reveals that the ideal scenario considerably overestimates the performance of the IS.

*A. Kaushik and F. K. Jondral are with Communications Engineering Lab, Karlsruhe Institute of Technology (KIT), Germany. Email:{ankit.kaushik,friedrich.jondral}@kit.edu}

†S.K. Sharma, S. Chatzinotas and B. Ottersten are with SnT - securityandtrust.lu, University of Luxembourg, Luxembourg. Email:{shree.sharma, symeon.chatzinotas, bjorn.ottersten}@uni.lu}.

A part of this paper has been presented at CROWNCOM 2015 in Doha, Qatar [1].

I. Introduction

We are currently in the phase of conceptualizing the requirements of the fifth-generation (5G) of wireless standards. One of the major requirements includes the improvement in the areal capacity (bits/s/m^2) by a factor of 1000 [2]. A large contribution of this demand is procured by means of an extension to the existing spectrum. Due to the static allocation of the spectrum specially below 6 GHz, which is appropriate for mobile communications, it is on the verge of scarcity. Given that the spectrum is utilized efficiently, it is possible to overcome this scarcity. In this perspective, cognitive radio is foreseen as one of the viable solutions that addresses the problem of spectrum scarcity.

An access to the Primary User (PU) spectrum is an outcome to the paradigm employed by the Secondary User (SU). Based on the paradigms described in the literature, all cognitive radio systems that deal dynamic access to the spectrum fall mainly under three categories namely, interweave, underlay and overlay systems [3]. As Interweave Systems (IS), the SUs render an interference-free access to the PU by exploiting spectral holes in different domains such as time, frequency, space and polarization existing in the licensed spectrum, whereas underlay systems enable an interference-tolerant access under which the SUs are allowed to use the licensed spectrum as long as they respect the interference constraints of the Primary Receivers (PRs). Besides that, overlay systems consider participation of higher layers for enabling spectral coexistence between two or more wireless networks. Due to its ease in deployment, IS is mostly preferred for performing analysis among these paradigms. In this context, this paper focuses on the performance analysis of the ISs from a deployment perspective.

Motivation and Related Work

Sensing is an integral part of the IS. At the Secondary Transmitter (ST), sensing is necessary for detecting the presence and absence of a primary signal, thereby protecting the PRs against harmful interference. Sensing at the ST is accomplished by listening to the signal transmitted by the PT. For detecting a primary signal, several techniques such as energy detection, matched filtering, cyclostationary and feature-based detection exist [4], [5]. Because of its versatility towards unknown primary signals and its low computational as well as deployment complexity requirement, energy detection has been extensively investigated in the literature [6]–[10]. According to energy detection, the decision is accomplished by comparing the power received at the ST to a threshold. In reality, the ST encounters variation in the received power due to existence of thermal noise at the receiver and fading in the channel. This leads to sensing errors described as misdetection or false alarm. These sensing errors limit the performance of the IS. Therefore, it is essential to characterize the expressions of probability of detection and probability of false alarm.

In particular, probability of detection is critical for the primary system because it precludes the PR from the interference induced by the ST. As a result, sustaining a desired value of probability of detection is of paramount importance to the secondary system [11]. Therefore, it is essential to characterize the probability of detection. Urkowitz [6] introduced a probabilistic model that establishes a fundamental framework for characterizing the sensing errors, however, the characterization accounted only noise in the system. Besides noise, fading in the channel causes further variation in the received power. To encounter this variation, different approaches has been investigated in the literature. Most prevalent approach involves an employment of a fading model. By this means, the variation in the received power is averaged out. Based on the underlying scenario, different fading models – Rice, Rayleigh, Nakagami-m and Log-normal can be employed [12]. The analytical expressions for the expected probability of detection for these models are characterized in [7]–[9].

Considering a cognitive radio system, this approach has some major drawbacks. Fading models depict a long-term characterization of the system, however, short-term interference that may lead to outage is ignored, thereby deteriorating the performance of primary system. Moreover, fading models are specific to the deployment scenario, hence, the knowledge of the fading model is necessary at system design. Apart from that, every fading model incurs certain model parameters. As a result, estimation of these parameters at the ST [13], particularly during the initial phase of the deployment, depicts an additional overhead. With this, a certain delay is imposed in the secondary system. In practice, due to mobility, most systems are likely to violate stationarity over a large duration. Thus, it becomes challenging to track these model parameters. As a consequence, these drawbacks constrict the applicability of this approach to practical cognitive radio systems.

To overcome these drawbacks, a different approach that exploits the channel coherence in time domain is established in [14]–[16]. In this regard, a frame structure is introduced such that the channel is considered to remain constant for the frame duration, however, upon exceeding the frame duration, the system may witness a different channel, hence, regarded as unknown. In this way, we preclude the variations due to the channel, thereby eluding the deployment of the fading model and model complexities thereafter. As a consequence, a short-term performance characterization of the IS is investigated, where the parameters are optimized for a given frame. In this paper, we focus on the latter approach.

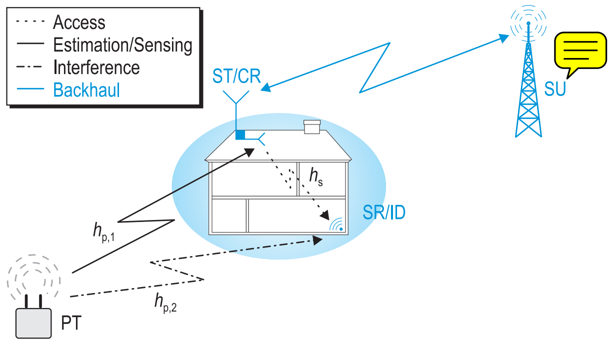

Fig. 1. A scenario demonstrating the interweave paradigm and the interacting channels.

Problem Formulation

Recently, the performance characterization of cognitive radio systems in terms of sensing-throughput tradeoff is getting a lot of attention [14], [16]–[18]. According to Liang *et al.* [14], the ST assures a reliable detection of primary signal, thereby sustaining the probability of detection above a desired level and simultaneously optimizes its throughputat the SR. The sensing-throughput tradeoff renders a suitable sensing time that achieves an optimum throughput for a given received power. However, to characterize the probability of detection and throughput, the system requires the knowledge of interacting channels. These include a sensing channel, an access channel and an interference channel, cf. Fig. 1. Several contributions investigated in the literature assume this knowledge to be present at the ST. As a result, the existing solutions are considered idealistic and implausible for deployment. The knowledge of these channels is not available in reality, thus, needs to be estimated at the ST. Unlike sensing channel, the access and interference channel has to be estimated at the SR and made available at the ST through a feedback channel.

Following the previous discussion, it is apparent that received power, that entails the sensing channel, is crucial for characterizing the probability of detection, hence, is essential in evaluating the detector's performance. With unknown channel, it is reasonable to include received power estimation for each frame [1]. Now, inherent to the estimation process, a variation is induced in the probability of detection. In this sense, characterizing the performance of detector with received power estimation remains an open problem. Besides probability of detection, probability of false alarm largely accounts for the throughput attained by the secondary system at the Secondary Receiver (SR). The characterization of the probability of false alarm requires the knowledge of noise power. Subject to a given uncertainty [19], this knowledge can be acquired through hardware calibration.

In order to breakthrough these bottlenecks, following solutions are proposed in the paper. Firstly, we consider received power estimation at the ST that allows us to constrain the probability of detection at a desired level. However, with the inclusion of estimation, the system anticipates: (i) a performance loss in terms of temporal resources used and (ii) a variation in the performance parameters due to estimation error. A preliminary analysis of this performance loss was done in [1], where, it was revealed that at low signal to noise ratio, imperfect estimation of received power results in large distortion in probability of detection, hence, cause a severe degradation in the performance of the IS. However, the performance degradation was determined by means of lower and upper bounds. Herein, we consider a more exact analysis, whereby we capture the variation in probability of detection by characterizing its distribution function. Using this, we apply new probabilistic constraints on the probability of detection that allow IS to operate at low signal to noise ratio.

Besides that, we include channel estimation at the SR to acquire the knowledge of the access and interference channels. It is well-known that systems with transmitter information (such as matched filter, pilot symbols, modulation type and time-frequency synchronization) at the receiver acquire channel knowledge by listening to the pilot data sent by the ST [20]–[23]. Other systems, where the receiver possess either no access to this information or limited by hardware complexity, procure channel knowledge indirectly by estimating a different parameter, for instance, received signal strength or received power, that entails the channel knowledge. Recently, pilot based estimation [24], [25] and received power estimation [26] have been applied to procure channel knowledge and depict the performance of cognitive systems. However, the analysis was restricted to underlay systems, where the emphasis was laid on modelling the interference at the PR. In this paper, we extend this notion to the IS, hence, employ pilot based estimation for the access channel and received power based estimation for the sensing and interference channels, cf. Fig. 1. Upon acquiring the knowledge of these channels at the ST, we depict the performance loss due to the estimation for the IS in terms of sensing-throughput tradeoff.

Contributions

The major contributions of the paper can be summarized as follows:

- The main goal of the paper is to establish a system model that constitutes channel estimation. With the inclusion of estimation, the system witnesses variation in the performance parameters and a certain performance loss. Based on the proposed model, this work investigates theses aspects and characterize the true performance of the IS.

- To capture the variation induced in the system, we characterize the distribution functions of performance parameters, the probability of detection and capacities at the SR. More importantly, we utilize the distribution function for the probability of detection to establish an average constraint or an outage constraint as new PU constraints on the probability of detection.
- Subject to the new constraints, we establish the expressions of sensing-throughput tradeoff . Based on these expressions, we depict the performance loss in terms of optimum throughput.
- Finally, we depict a fundamental tradeoff between estimation time, sensing time and throughput. We exploit this tradeoff to determine a suitable estimation and sensing time that depicts an optimal performance of the IS.

Organization

The subsequent sections of the paper are organized as follows: Section II describes the system model that includes the interweave scenario, the signal model and performance characterization for the ideal scenario. Section III presents the proposed model that characterizes the distribution functions of the performance parameters. Moreover, it establishes the sensing-throughput tradeoff subject to average and outage constraints. Section IV analyzes the numerical results based on the obtained expressions. Finally, Section V concludes the paper.

II. System Model

Interweave scenario

Cognitive Relay (CR) [27] characterizes a small cell deployment that fulfills the spectral requirements for Indoor Devices (IDs). Fig. 1 illustrates a snapshot of a CR scenario to depict the interaction between the CR with PT and ID, where CR and ID represents the ST and SR respectively. In [27], the challenges involved while deploying the CR as an IS were presented. For simplification, a PU constraint based on probability of false alarm rate was considered in the system model. With the purpose of improving reliability of the system, we extend the analysis to employ a PU constraint on the probability of detection. We consider a slotted medium access for the IS, where the time axis is segmented into frames of length T [14]. According to which, the ST employs periodic sensing, hence, each frame consists of a sensing slot τ_{sen} and the remaining duration $T - \tau_{\text{sen}}$ is utilized for data transmission. For small T relative to the PU's expected ON/OFF period, the requirement of the ST to be in alignment to PUs' medium access can be relaxed [28]–[30].

TABLE I

DEFINITIONS OF ACRONYMS AND NOTATIONS USED

Acronyms and Notations	Definitions
AC, OC	Average Constraint, Outage Constraint
CR	Cognitive Relay
IM,EM	Ideal Model, Estimation Model
IS	Interweave System
PU - PT, PR	Primary User - Primary Transmitter, Primary Receiver
SU - ST, SR	Secondary User - Secondary Transmitter, Secondary Receiver
$\mathcal{H}_1, \mathcal{H}_0$	Signal plus noise Hypothesis, noise only hypothesis
$f_{\rm s}$	Sampling frequency
$\tau_{\rm est}, \tau_{\rm sen}$	Estimation time, sensing time interval
T	Frame duration
$\rm P_d, P_{fa}$	Probability of detection, probability of false alarm
$\rm \bar{P}_d$	Constraint over probability of detection
κ	Outage Constraint over probability of detection
$h_{\rm p,1}, h_{\rm p,2}, h_{\rm s}$	Channel coefficient for the link PT-ST, PT-SR, ST-SR
$\gamma_{\rm p,1}, \gamma_{\rm p,2}, \gamma_{\rm s}$	Signal to noise ratio for the link PT-ST, PT-SR, ST-SR
$R_{\rm s}$	Throughput at SR
$\rm C_0, C_1$	Shanon capacity at SR without and with interference from PT
μ	Threshold for the energy detector
$F_{(\cdot)}$	Cumulative distribution function of random variable $(\cdot)$
$f_{(\cdot)}$	Probability density function of random variable $(\cdot)$
$\hat{(\cdot)}$	Estimated value of $(\cdot)$
$\tilde{(\cdot)}$	Optimum value of $(\cdot)$
$\mathbb{E}_{(\cdot)}$	Expectation with respect $(\cdot)$
$\mathbb{P}$	Probability measure
$\mathbf{T}(\cdot)$	Test statistics
$x_{(\cdot)}[n], y_{(\cdot)}[n]$	$n^{\rm th}$ sample of the transmitted discrete signal, received discrete signal at $(\cdot)$
$P_{{\rm Tx},\,(\cdot)}, P_{{\rm Rx},\,(\cdot)}$	Power transmitted, power received at $(\cdot)$
σ_x^2, σ_w^2	Signal variance at PT, noise variance at ST and SR
$\Gamma(\cdot)$	Gamma function
$\Gamma(\cdot,\cdot)$	Regularized incomplete upper Gamma function
$\Gamma^{-1}(\cdot,\cdot)$	Inverse of regularized incomplete upper Gamma function
$\mathcal{N}, \mathcal{X}^2, \mathcal{X}_1^2$	Normal, central chi-squared, non-central chi-squared distribution
$N_{\rm s}$	Number of pilot symbols used for pilot based estimation at the SR for $h_{\rm s}$
$N_{\rm p,2}$	Number of samples used for received power estimation at the SR for $h_{\rm p,2}$
a_1, b_1, a_2, b_2	Model parameters of Gamma distribution
λ	Non-centrality parameter of $\mathcal{X}_1^2$ distribution

Signal model

The discrete signal received illustrating the presence $(\mathcal{H}_1)$ or absence $(\mathcal{H}_0)$ of a primary signal is given by

$$y_{\mathrm{ST}}[n] = \begin{cases} h_{\mathrm{p},1} \cdot x_{\mathrm{PT}}[n] + w[n] & : \mathcal{H}_1 \\ w[n] & : \mathcal{H}_0 \end{cases}, \tag{1}$$

where $x_{\mathrm{PT}}[n]$ corresponds to a discrete sample transmitted by the PT, $|h_{\mathrm{p},1}|^2$ represents the power gain for the channel for a given frame and $w[n]$ is additive white Gaussian Noise (AWGN) at the ST. The primary signal $x_{\mathrm{PT}}[n]$ can be modelled as: (i) PSK modulated signal, or (ii) Gaussian signal. The signals that are prone to high inter symbol interference or entail precoding can be modelled as Gaussian signal [14]. For this paper, we focus our analysis on the latter case. As a result, the mean and variance for the signal and noise are determined as $\mathbb{E}\left[x_{\mathrm{PT}}[n]\right] = 0$, $\mathbb{E}\left[w[n]\right] = 0$, $\mathbb{E}\left[|x_{\mathrm{PT}}[n]|^2\right] = \sigma_x^2$ and $\mathbb{E}\left[|w[n]|^2\right] = \sigma_w^2$. The channel $h_{\mathrm{p},1}$ is considered to be independent to $x_{\mathrm{PT}}[n]$ and $w[n]$, thus, y_{ST} is also an i.i.d. random process.

Similar to (1), during data transmission, the discrete received signal at the SR conditioned over the probability of detection ($\mathrm{P_d}$) and probability of false alarm ($\mathrm{P_{fa}}$) is given by

$$y_{\mathrm{SR}}[n] = \begin{cases} h_{\mathrm{s}} \cdot x_{\mathrm{ST}}[n] + h_{\mathrm{p},2} \cdot x_{\mathrm{PT}}[n] + w[n] & : 1 - \mathrm{P_d} \\ h_{\mathrm{s}} \cdot x_{\mathrm{ST}}[n] + w[n] & : 1 - \mathrm{P_{fa}} \end{cases}, \tag{2}$$

where $x_{\mathrm{ST}}[n]$ corresponds to discrete signal transmitted by the ST. Further, $|h_{\mathrm{s}}|^2$ and $|h_{\mathrm{p},2}|^2$ represent the power gains for channel, cf. Fig. 1.

Sensing

Following the frame structure, ST performs sensing for a duration of τ_{sen}, cf. Fig. 2. The test statistics $\mathrm{T}(\mathbf{y})$ at the ST is evaluated as

$$\mathrm{T}(\mathbf{y}) = \frac{1}{\tau_{\mathrm{sen}} f_{\mathrm{s}}} \sum_{n}^{\tau_{\mathrm{sen}} f_{\mathrm{s}}} |y_{\mathrm{ST}}[n]|^2 \underset{\mathcal{H}_0}{\overset{\mathcal{H}_1}{\gtrless}} \mu, \tag{3}$$

where μ is the threshold and $\mathbf{y}$ is a vector with $\tau_{\mathrm{sen}} f_{\mathrm{s}}$ samples. $\mathrm{T}(\mathbf{y})$ represents a random variable, whereby the characterization of the distribution function depends on the underlying hypothesis. Corresponding to $\mathcal{H}_0$ and $\mathcal{H}_1$, $\mathrm{T}(\mathbf{y})$ follows a central chi-squared ($\mathcal{X}^2$) distribution [31]. As a result, the probability of detection $\mathrm{P_d}$ and the probability of false alarm $\mathrm{P_{fa}}$ corresponding to (3) is determined as [19]

$$\mathrm{P_d}(\mu, \tau_{\mathrm{sen}}, P_{\mathrm{Rx,ST}}) = \Gamma\left(\frac{\tau_{\mathrm{sen}} f_{\mathrm{s}}}{2}, \frac{\tau_{\mathrm{sen}} f_{\mathrm{s}} \mu}{2 P_{\mathrm{Rx,ST}}}\right), \tag{4}$$

$$\mathrm{P_{fa}}(\mu, \tau_{\mathrm{sen}}) = \Gamma\left(\frac{\tau_{\mathrm{sen}} f_{\mathrm{s}}}{2}, \frac{\tau_{\mathrm{sen}} f_{\mathrm{s}} \mu}{2\sigma_w^2}\right), \tag{5}$$

where $\Gamma(\cdot,\cdot)$ represents a regularized upper Gamma function [32].

Sensing-Throughput tradeoff

Following the characterization of $\mathrm{P_{fa}}$ and $\mathrm{P_d}$, Liang *et. al.* [14] established a tradeoff between the sensing time and secondary throughput (R_{s}) attained subject to a desired probability of detection $\bar{\mathrm{P}}_{\mathrm{d}}$. This tradeoff is represented as

$$\tilde{R}_{\mathrm{s}}(\tilde{\tau}_{\mathrm{sen}}) = \max_{\tau_{\mathrm{sen}}} R_{\mathrm{s}}(\tau_{\mathrm{sen}}) = \frac{T - \tau_{\mathrm{sen}}}{T}\Bigg[\mathrm{C}_0(1 - \mathrm{P_{fa}})\mathbb{P}(\mathcal{H}_0) + \mathrm{C}_1(1 - \mathrm{P_d})\mathbb{P}(\mathcal{H}_1)\Bigg], \tag{6}$$

$$\text{s.t. } \mathrm{P_d} \geq \bar{\mathrm{P}}_{\mathrm{d}}, \tag{7}$$

$$\text{where } \mathrm{C}_0 = \log_2\left(1 + |h_{\mathrm{s}}|^2 \frac{P_{\mathrm{Tx,ST}}}{\sigma_w^2}\right) = \log_2(1 + \gamma_{\mathrm{s}}) \tag{8}$$

$$\text{and } \mathrm{C}_1 = \log_2\left(1 + \frac{|h_{\mathrm{s}}|^2 P_{\mathrm{Tx,ST}}}{|h_{\mathrm{p,2}}|^2 P_{\mathrm{Tx,PT}} + \sigma_w^2}\right) = \log_2\left(1 + \frac{|h_{\mathrm{s}}|^2 P_{\mathrm{Tx,ST}}}{P_{\mathrm{Rx,SR}}}\right) = \log_2\left(1 + \frac{\gamma_{\mathrm{s}}}{\gamma_{\mathrm{p,2}} + 1}\right). \tag{9}$$

$\mathbb{P}(\mathcal{H}_0)$ and $\mathbb{P}(\mathcal{H}_1)$ are the probabilities of occurrence for the respective hypothesis, whereas $\gamma_{\mathrm{p,2}}$ and γ_{s} corresponds to signal to noise ratio for the links PT-SR and SR-SR, respectively. In other words, using (6), the ST determines a suitable sensing time $\tau_{\mathrm{sen}} = \tilde{\tau}_{\mathrm{sen}}$, such that the throughput is optimized $\tilde{R}_{\mathrm{s}}$ subject to a desired probability of detection, cf. (7). From the deployment perspective, the tradeoff depicted above has fundamental issues:

- Without the knowledge of the received power (sensing channel), it is not feasible to characterize $\mathrm{P_d}$. This further leaves the characterization of the throughput (6) impossible and the constraint defined in (7) invalid.
- Moreover, the knowledge of the interacting channels is required at the ST, cf. (8) and (9) for characterizing the throughput in terms of C_0 and C_1 at the SR.

With these issues, it is unreasonable to depict the performance of IS based on such characterization. In the subsequent section, we propose an estimation model that complements these issues, thereby including the estimation of the sensing channel at the ST and interference and access channel at the SR. Based on the proposed model, we then investigate the performance of the IS.

III. Proposed Model

The inclusion of estimation of the interacting channels causes variation in the parameters $\mathrm{P_d}$, C_0 and C_1. Unless characterized, this variation may be hazardous for a hardware deployment. In this view, we

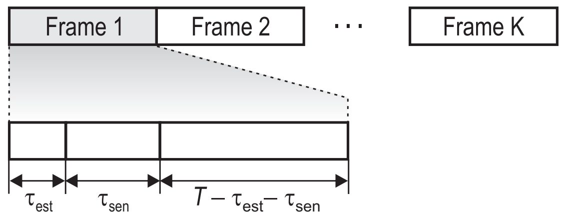

Fig. 2. Frame structure of interweave system with received power estimation.

include the estimation of the interacting channels in the system model, thereby characterizing the variation in $\mathrm{P_d}$, $\mathrm{C_0}$ and $\mathrm{C_1}$ by means of distribution functions. Equipped with these expressions, we finally obtain a characterization of sensing-throughput tradeoff. To include channel estimation, we propose a frame structure includes estimation τ_{est}, sensing τ_{sen} and data transmission $T - (\tau_{\text{est}} + \tau_{\text{sen}})$, where $\tau_{\text{est}}, \tau_{\text{sen}}$ correspond to time intervals and $\tau_{\text{est}} + \tau_{\text{sen}} < T$, cf. Fig. 2. In this context, the estimation of the channels is dealt in the following sub-sections.

Estimation of sensing channel ($h_{p,1}$)

Following previous discussions, the ST acquires the knowledge of $h_{\text{p},1}$ by estimating its received power. The estimated received power is required for the characterization of $\mathrm{P_d}$, thereby evaluating the detector performance.

Under $\mathcal{H}_1$, the received power estimated in the estimation phase at the ST is given as [6]

$$\hat{P}_{\text{Rx,ST}} = \frac{1}{\tau_{\text{est}} f_{\text{s}}} \sum_{n}^{\tau_{\text{est}} f_{\text{s}}} |y_{\text{ST}}[n]|^2. \tag{10}$$

$\hat{P}_{\text{Rx,ST}}$ determined in (10) using $\tau_{\text{est}} f_{\text{s}}$ samples follows a central chi-squared distribution $\mathcal{X}^2$ [31]. The distribution function of $\hat{P}_{\text{Rx,ST}}$ is given by

$$F_{\hat{P}_{\text{Rx,ST}}}(x) = 1 - \Gamma\left(\frac{\tau_{\text{est}} f_{\text{s}}}{2}, \frac{\tau_{\text{est}} f_{\text{s}} x}{2 P_{\text{Rx,ST}}}\right). \tag{11}$$

Estimation of access channel (h_s)

The signal received from the ST undergoes matched filtering and demodulation at the SR, hence, it is reasonable to employ pilot based estimation for h_{s}. Unlike received power estimation, pilot based estimation renders a direct estimation of the channel. Now, to accomplish pilot based estimation, the SR aligns itself to pilot symbols transmitted by the ST. Without loss of generality, the pilot symbols are considered to be +1. Under $\mathcal{H}_1$, the discrete pilot symbols at the output of the demodulator is given by [22]

$$p[n] = \sqrt{E_{\mathrm{s}}} h_{\mathrm{s}} + w[n], \tag{12}$$

where E_{s} denotes the pilot energy. The maximum likelihood estimate, representing a sample average of N_{s} pilot symbols, is given by [21]

$$h_{\mathrm{s}} = \hat{h}_{\mathrm{s}} + \underbrace{\frac{\sum_i^{N_{\mathrm{s}}} n[i]}{2\sqrt{E_{\mathrm{s}}} N_{\mathrm{s}}}}_{\epsilon}, \tag{13}$$

where ϵ denotes the estimation error. The estimate $\hat{h}_{\mathrm{s}}$ is unbiased, efficient and achieves a Cramer-Rao bound with equality, with variance $\mathbb{E}\left[|h_{\mathrm{s}} - \hat{h}_{\mathrm{s}}|^2\right] = \sigma_w^2/(2E_{\mathrm{s}}N_{\mathrm{s}})$ [22]. Consequently, $\hat{h}_{\mathrm{s}}$ conditioned on h_{s} follows a Gaussian distribution

$$\hat{h}_{\mathrm{s}} | h_{\mathrm{s}} \sim \mathcal{N}\left(h_{\mathrm{s}}, \frac{\sigma_w^2}{2E_{\mathrm{s}}N_{\mathrm{s}}}\right) \tag{14}$$

As a result, the power gain $|\hat{h}_{\mathrm{s}}|^2$ follows a non-central chi-squared ($\mathcal{X}_1^2$) distribution with 1 degree of freedom and non-centrality parameter $\lambda = \frac{|h_{\mathrm{s}}|^2}{\frac{\sigma_w^2}{2E_{\mathrm{s}}N_{\mathrm{s}}}}$.

Estimation of interference channel ($h_{p,2}$)

In addition, analog to sensing channel, the SR performs received power estimation by listening to the transmission from the PT. The knowledge of $h_{\mathrm{p},2}$ is required to characterize interference from the PT. Under $\mathcal{H}_0$, the discrete signal model at the SR is given as

$$y_{\mathrm{SR}}[n] = h_{\mathrm{p},2} \cdot x_{\mathrm{PT}}[n] + w[n]. \tag{15}$$

Analog to $\hat{P}_{\mathrm{Rx,ST}}$, the received power at the SR from the PT given by

$$\hat{P}_{\mathrm{Rx,SR}} = \frac{1}{N_{\mathrm{p},2}} \sum_{n}^{N_{\mathrm{p},2}} |y_{\mathrm{SR}}[n]|^2, \tag{16}$$

follows a $\mathcal{X}^2$ distribution, where $N_{\mathrm{p},2}$ corresponds to the number of samples used for estimation.

Assumptions and Approximations

To simplify the analysis and sustain analytical tractability for the proposed model, several assumptions are considered in the paper are summarized as follows:

- We consider that all transmitted signals are subjected to distance dependent path loss and small scale fading gain. With no loss of generality, we consider that the channel gains include distance dependent path loss and small scale gain. Moreover, Moreover, the coherence time for the channel gain is greater than the frame duration. However, we may still encounter scenarios where the coherence time exceeds the frame duration, in such cases our characterization depicts a lower performance bound.

- We consider disjoint sets of samples for estimation and sensing for a certain frame. However, in practice, it is possible to utilize the samples used in the estimation phase for sensing purpose as well, which leads to an improvement in the performance in terms of the number of samples utilized for sensing.
- We assume perfect knowledge of the noise. The uncertainty in the noise power can be captured as a bounded interval [19]. Inserting this interval in expressions obtained, it is possible to express of the performance in terms of best and worst bounds.
- For all degrees of freedom, $\mathcal{X}_1^2$ distribution can be approximated as Gamma distribution [33]. The parameters of the Gamma distribution are computed by comparing its first two central moments with that of $\mathcal{X}_1^2$.
- The signal model constituting channel estimation, stipulates the knowledge of the underlying hypothesis at the ST and the SR. Upon the application of PU traffic models proposed in [28]–[30], it is possible to acquire this knowledge with high probability. Moreover, it is reasonable that the ST and the SR performs estimation independently. Considering a realistic situation, it is possible that SR doesn't accomplish estimation in each frame. In this context, the ST utilizes the previous estimation value for the analysis.
- Finally, it is assumed that the estimation time for the channels h_{s} and $h_{\mathrm{p},2}$ is smaller than $h_{\mathrm{p},1}$, that is $N_{\mathrm{p},2}, N_{\mathrm{s}} < \tau_{\mathrm{sen}} f_{\mathrm{s}}$. Hence, it is sufficient to incorporate $\max(\tau_{\mathrm{est}} f_{\mathrm{s}}, N_{\mathrm{s}}, N_{\mathrm{p},2}) = \tau_{\mathrm{est}}$ in the expression of the throughput.

Now, the variation due to the estimation of the channels translates to the variation of the performance parameters $\mathrm{P_d}, \mathrm{C_0}, \mathrm{C_1}$, that form the basis of the sensing-throughput tradeoff. We capture this variation by characterizing their distribution functions $F_{\mathrm{P_d}}$, $F_{\mathrm{C_0}}$ and $F_{\mathrm{C_1}}$. By means of simulations, we validate the theoretical expressions obtained.

Lemma 1: The distribution function of $\mathrm{P_d}$ is characterized as

$$F_{\mathrm{P_d}}(x) = 1 - \Gamma\left(\frac{\tau_{\mathrm{est}} f_{\mathrm{s}}}{2}, \frac{\tau_{\mathrm{est}} f_{\mathrm{s}} \tau_{\mathrm{sen}} f_{\mathrm{s}} \mu}{4 P_{\mathrm{Rx,ST}} \Gamma^{-1}\left(\frac{\tau_{\mathrm{sen}}}{2}, x\right)}\right) \tag{17}$$

where $\Gamma^{-1}(\cdot,\cdot)$ is inverse function of regularized upper Gamma function [32].

(a) $\tau_{\text{est}} \in \{1, 5, 10\}$ms and $\tau_{\text{sen}} = 1$ ms (b) $\tau_{\text{est}} = 5$ ms and $\tau_{\text{sen}} \in \{1, 5, 10\}$ms

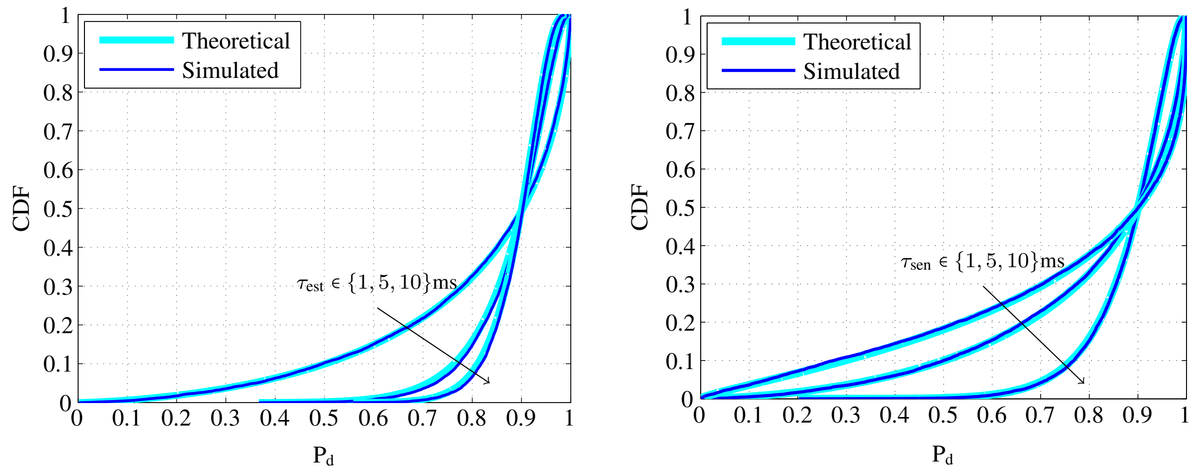

Fig. 3. CDF of P_d for different τ_{est} and τ_{sen}.

Proof: The distribution function of P_d is defined as

$$F_{\text{P}_\text{d}}(x) = \mathbb{P}(\text{P}_\text{d} \leq x) \tag{18}$$

Using (4)

$$= \mathbb{P}\left(\Gamma\left(\frac{\tau_{\text{sen}} f_\text{s}}{2}, \frac{\tau_{\text{est}} f_\text{s} \mu}{2\hat{P}_{\text{Rx,ST}}}\right) \leq x\right) \tag{19}$$

$$= 1 - \mathbb{P}\left(\hat{P}_{\text{Rx,ST}} \leq \frac{\mu \tau_{\text{sen}} f_\text{s}}{2\Gamma^{-1}\left(\frac{\tau_{\text{sen}} f_\text{s}}{2}, x\right)}\right) \tag{20}$$

Replacing the distribution function of $\hat{P}_{\text{Rx,ST}}$ in (20), we obtain an expression of F_{P_d}. ■

From (17), it is clearly observed that F_{P_d} depends on $P_{\text{Rx,ST}}$, τ_{sen} and τ_{est}.

Lemma 2: The distribution function of C_0 is defined as

$$F_{\text{C}_0}(x) = \int_0^\infty f_{\text{C}_0}(x) dx, \tag{21}$$

where

$$f_{\text{C}_0}(x) = 2^x \ln 2 \frac{(2^x - 1)^{a_1 - 1}}{\Gamma(a_1) b_1^{a_1}} \exp\left(-\frac{2^x - 1}{b_1}\right), \tag{22}$$

and

$$a_1 = \frac{\left(\frac{\sigma_w^2}{2E_\text{s}N_\text{s}} \frac{\sigma_w^2}{P_{\text{Tx,ST}}} + |h_\text{s}|^2\right)^2}{\frac{\sigma_w^2}{2E_\text{s}N_\text{s}} \frac{\sigma_w^2}{P_{\text{Tx,ST}}} \left(2\frac{\sigma_w^2}{2E_\text{s}N_\text{s}} \frac{\sigma_w^2}{P_{\text{Tx,ST}}} + 4|h_\text{s}|^2\right)} \text{ and } b_1 = \frac{\frac{\sigma_w^2}{2E_\text{s}N_\text{s}} \frac{\sigma_w^2}{P_{\text{Tx,ST}}} \left(2\frac{\sigma_w^2}{2E_\text{s}N_\text{s}} \frac{\sigma_w^2}{P_{\text{Tx,ST}}} + 4|h_\text{s}|^2\right)}{\left(\frac{\sigma_w^2}{2E_\text{s}N_\text{s}} \frac{\sigma_w^2}{P_{\text{Tx,ST}}} + |h_\text{s}|^2\right)}. \tag{23}$$

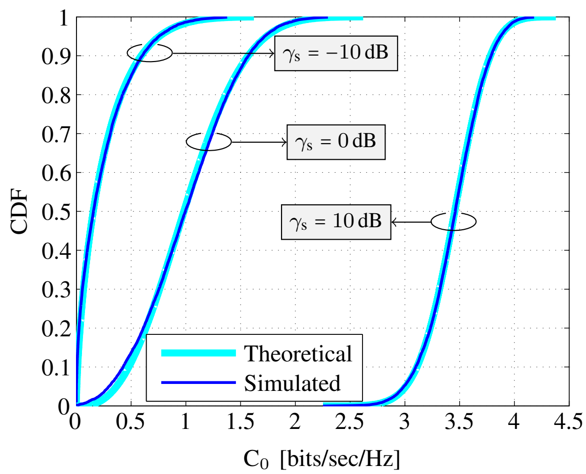

Fig. 4. CDF of C_0 for different values of $\gamma_s \in \{-10, 0, 10\}$dB.

Proof: Following the pdf of $|\hat{h}_s|^2$ in (14), the pdf $|\hat{h}_s|^2 \frac{P_{Tx,ST}}{\sigma_w^2}$ is given by

$$f_{\frac{|\hat{h}_s|^2 P_{Tx,ST}}{\sigma_w^2}}(x) = \frac{P_{Tx,ST}}{\sigma_w^2} \frac{1}{\frac{\sigma_w^2}{2E_s N_s}} \frac{1}{2} \exp\left[-\frac{1}{2}\left(x \frac{\sigma_w^2}{2E_s N_s} \frac{\sigma_w^2}{P_{Tx,ST}} + \lambda\right)\right] \left(\frac{x \frac{\sigma_w^2}{2E_s N_s}}{\lambda} \frac{\sigma_w^2}{P_{Tx,ST}}\right)^{\frac{N_s}{4} - \frac{1}{2}} I_{\frac{N_s}{2}-1}\left(\sqrt{\lambda x \frac{\sigma_w^2}{2E_s N_s} \frac{\sigma_w^2}{P_{Tx,ST}}}\right)$$

Approximating $\mathcal{X}_1^2(\cdot,\cdot)$ with Gamma distribution $\Gamma(a_1, b_1)$ gives [33]

$$f_{\frac{|\hat{h}_s|^2 P_{Tx,ST}}{\sigma_w^2}} \approx \frac{1}{\Gamma(a_1)} \frac{x^{a_1 - 1}}{b_1^{a_1}} \exp\left(-\frac{x}{b_1}\right), \tag{24}$$

where the parameters a_1, b_1 are determined by comparing the first two central moments of the two distribution. Finally, by substituting the expression of C_0 in (8) yields (22). ■

Lemma 3: The distribution function of C_1 is given by

$$F_{C_1}(x) = \int_0^\infty f_{C_1}(x) dx, \tag{25}$$

where

$$f_{C_1}(x) = 2^x \ln 2 \frac{(2^x - 1)^{a_1 - 1} \Gamma(a_1 + a_2)}{\Gamma(a_1)\Gamma(a_2) b_1^{a_1} b_2^{a_2}} \left(\frac{1}{b_2} + \frac{2^x - 1}{b_1}\right), \tag{26}$$

and

$$a_2 = \frac{N_{p,2}}{2} \text{ and } b_2 = \frac{2 P_{Rx,ST}}{\sigma_w^2 N_{p,2}}, \tag{27}$$

where a_1 and b_1 are defined in (23).

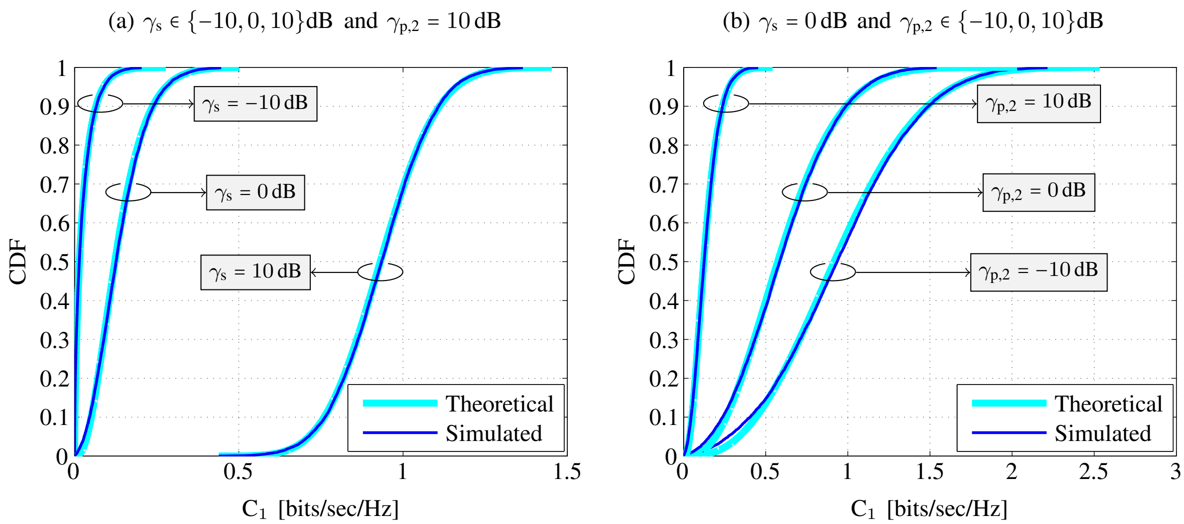

Fig. 5. CDF of C_1 for different γ_s and $\gamma_{p,2}$.

Proof: For simplification, we disintegrate the expression $\left(\frac{|\hat{h}_s|^2 P_{\text{Tx,ST}}}{\hat{P}_{\text{Rx,SR}}}\right)$ in (9), as $E_1 = \left(\frac{|\hat{h}_s|^2 P_{\text{Tx,ST}}}{\sigma_w^2}\right)$ and $E_2 = \left(\frac{\hat{P}_{\text{Rx,SR}}}{\sigma_w^2}\right)$, where $\text{C}_1 = \log_2\left(1 + \frac{E_1}{E_2}\right)$.

Now, following the characterization $\hat{P}_{\text{Rx,SR}}$ in (16), the pdf of E_2 is determined as

$$f_{\frac{\hat{P}_{\text{Rx,SR}}}{\sigma_w^2}} = \frac{N_{p,2}\sigma_w^2}{P_{\text{Rx,ST}}} \frac{1}{2^{\frac{N_{p,2}}{2}} \Gamma\left(\frac{N_{p,2}}{2}\right)} \left(x \frac{N_{p,2}\sigma_w^2}{P_{\text{Rx,ST}}}\right)^{\frac{N_{p,2}}{2}-1} \exp\left(-x \frac{N_{p,2}\sigma_w^2}{2P_{\text{Rx,ST}}}\right). \tag{28}$$

The pdf of the expression E_1 is determined in (24).

Using the characterizations of pdfs $f_{\frac{|\hat{h}_s|^2 P_{\text{Tx,ST}}}{\sigma_w^2}}$ and $f_{\frac{\hat{P}_{\text{Rx,SR}}}{\sigma_w^2}}$, we apply Mellin transform [34] to determine the pdf of $\frac{E_1}{E_2}$ as

$$f_{\frac{|\hat{h}_s|^2 P_{\text{Tx,ST}}}{\sigma_w^2} \Big/ \frac{\hat{P}_{\text{Rx,SR}}}{\sigma_w^2}}(x) = \frac{x^{a_1-1}\Gamma(a_1+a_2)}{\Gamma(a_1)\Gamma(a_2) b_1^{a_1} b_2^{a_2}} \left(\frac{1}{b_2} + \frac{x}{b_1}\right). \tag{29}$$

Finally, substituting the expression $\frac{E_1}{E_2}$ in C_1 yields (26). ■

Sensing-throughput tradeoff

Here, we establish sensing-throughput tradeoff for the estimation model that includes estimation time and incorporates variation in the performance parameter. Most importantly, by capturing this variation , we establish two new primary user constraints at the PR, namely, an average constraint and an outage constraint on the probability of detection. These constraints constrict the harmful interference at the PR.

Based on these constraints and estimation time τ_{est}, we characterize the sensing-throughput tradeoff for the IS.

Theorem 1: Subject to an average constraint on $\mathrm{P_d}$ at the PR, the sensing-throughput tradeoff is given by

$$\tilde{R}_{\text{s}}(\tilde{\tau}_{\text{sen}}) = \max_{\tau_{\text{sen}}} \mathbb{E}_{\mathrm{P_d},\mathrm{C_0},\mathrm{C_1}}\left[R_{\text{s}}(\tau_{\text{sen}})\right] = \frac{T-\tau_{\text{sen}}-\tau_{\text{est}}}{T}\Bigg[\mathbb{E}_{\mathrm{C_0}}\left[\mathrm{C_0}\right](1-\mathrm{P_{fa}})\mathbb{P}(\mathcal{H}_0)+$$
$$\mathbb{E}_{\mathrm{C_1}}\left[\mathrm{C_1}\right](1-\mathbb{E}_{\mathrm{P_d}}\left[\mathrm{P_d}\right])\mathbb{P}(\mathcal{H}_1)\Bigg], \tag{30}$$

$$\text{s.t. } \mathbb{E}_{\mathrm{P_d}}\left[\mathrm{P_d}\right] \le \bar{\mathrm{P}}_{\mathrm{d}}. \tag{31}$$

$\mathbb{E}_{\mathrm{P_d}}\left[\cdot\right]$ represents the expectation with respect to $\mathrm{P_d}$, $\mathbb{E}_{\mathrm{P_d},\mathrm{C_0},\mathrm{C_1}}\left[\cdot\right]$ denotes the expectation with respect to $\mathrm{P_d}$, $\mathrm{C_0}$ and $\mathrm{C_1}$. Unlike (7), $\bar{\mathrm{P}}_{\mathrm{d}}$ in (30) represents the constraint on expected probability of detection.

Theorem 2: Subject to an outage constraint on $\mathrm{P_d}$ at the PR, the sensing-throughput tradeoff is given by

$$\tilde{R}_{\text{s}}(\tilde{\tau}_{\text{sen}}) = \max_{\tau_{\text{sen}}} \mathbb{E}_{\mathrm{P_d},\mathrm{C_0},\mathrm{C_1}}\left[R_{\text{s}}(\tau_{\text{sen}})\right] = \frac{T-\tau_{\text{sen}}-\tau_{\text{est}}}{T}\Bigg[\mathbb{E}_{\mathrm{C_0}}\left[\mathrm{C_0}\right](1-\mathrm{P_{fa}})\mathbb{P}(\mathcal{H}_0)+$$
$$\mathbb{E}_{\mathrm{C_1}}\left[\mathrm{C_1}\right](1-\mathbb{E}_{\mathrm{P_d}}\left[\mathrm{P_d}\right])\mathbb{P}(\mathcal{H}_1)\Bigg], \tag{32}$$

$$\text{s.t. } \mathbb{P}(\mathrm{P_d} \le \bar{\mathrm{P}}_{\mathrm{d}}) \le \kappa, \tag{33}$$

where κ represents the outage constraint.

In order to solve the constrained optimization problems illustrated in Theorem 1 and Theorem 2, the following approach is considered. As a first step, an underlying constraint is employed to determine μ as a function of the τ_{sen} and τ_{est}. Its value is substituted in (4) and (5) to determine $\mathrm{P_{fa}}$ and $\mathrm{P_d}$. Finally, replacing $\mathrm{P_d}$ and $\mathrm{P_{fa}}$ inside (30) and (32), we obtain an expression of the throughput in terms of τ_{sen}, τ_{est} and the system parameters. Using this expression, we consider the variation of expected throughput along τ_{est} and τ_{sen}, thereby determining an optimum throughput.

Corollary 1: For the average constraint, the analytical expression $\mathbb{E}_{\mathrm{P_d}}\left[\mathrm{P_d}\right]$ did not lead to a closed form expression. In this context, we procure the threshold μ for the average constraint numerically.

Corollary 2: For this case, we determine the threshold μ based on the outage constraint. This is accomplished by combining the expression of $F_{\mathrm{P_d}}$ in (17) with the outage constraint (33)

$$P(\mathrm{P_d} \le \bar{\mathrm{P}}_{\mathrm{d}}) = F_{\mathrm{P_d}}(\bar{\mathrm{P}}_{\mathrm{d}}) \le \kappa. \tag{34}$$

Rearranging (34) gives

$$\mu \geq \frac{4P_{\mathrm{Rx,ST}}\Gamma^{-1}\left(1-\kappa, \frac{\tau_{\mathrm{est}} f_{\mathrm{s}}}{2}\right)\Gamma^{-1}\left(1-\bar{\mathrm{P}}_{\mathrm{d}}, \frac{\tau_{\mathrm{sen}} f_{\mathrm{s}}}{2}\right)}{\tau_{\mathrm{est}} f_{\mathrm{s}} \tau_{\mathrm{sen}} f_{\mathrm{s}}} \tag{35}$$

Upon replacing the respective thresholds in $\mathrm{P_d}$ and $\mathrm{P_{fa}}$ and evaluating the expectation over $\mathrm{P_d}$, $\mathrm{C_0}$ and $\mathrm{C_1}$ using Lemma 1, Lemma 2 and Lemma 3, we determine the expected throughput as a function of sensing and estimation time. As a consequence, by fixing the estimation time, sensing-throughput tradeoff that depicts the variation of expected throughput against the sensing time is established based on the average and outage constraint. In contrast to the ideal model, the sensing-throughput tradeoff substantiated by the estimation model incorporates the channel knowledge is qualified for characterizing the performance of IS.

Corollary 3: Subsequently, following the variation of optimum expected throughput $\tilde{R}_{\mathrm{s}}(\tau_{\mathrm{est}}, \tilde{\tau}_{\mathrm{sen}})$ (optimized over the sensing time) against the estimation time, we depict an estimation-sensing-throughput tradeoff. Based on this, we determine the suitable estimation $\tau_{\mathrm{est}} = \tilde{\tau}_{\mathrm{est}}$ and sensing time that achieves an optimum throughput $\tilde{R}_{\mathrm{s}}(\tilde{\tau}_{\mathrm{est}}, \tilde{\tau}_{\mathrm{sen}})$ for the IS.

IV. Numerical Analysis

Here, we investigate the performance of the IS based on the proposed model. To accomplish this: (i) we perform simulations to validate the expressions obtained, (ii) we analyze the performance loss incurred due to the estimation. In this regard, we consider the ideal model for benchmarking and evaluating the performance loss, (iii) we establish mathematical justification to the considered approximations. Although, the expressions derived using our sensing-throughput analysis are general and applicable to all cognitive radio systems, however, the parameters are selected in such a way that they closely relate to the deployment scenario described in Fig. 1. Unless stated explicitly, the following choice of the parameters is considered for the analysis, $f_{\mathrm{s}} = 1\,\mathrm{MHz}$, $h_{\mathrm{p},1} = h_{\mathrm{p},2} = -100\,\mathrm{dB}, h_{\mathrm{s}} = -80\,\mathrm{dB}$, $T = 100\,\mathrm{ms}$, $\bar{\mathrm{P}}_{\mathrm{d}} = 0.9$, $\kappa = 0.05$ $\sigma_w^2 = -100\,\mathrm{dBm}$, $\gamma_{\mathrm{p},1} = -10\,\mathrm{dB}$, $\gamma_{\mathrm{p},2} = -10\,\mathrm{dB}$, $\gamma_{\mathrm{s}} = 10\,\mathrm{dB}$, $\sigma_x^2 = P_{\mathrm{Tx,PT}} = -10\,\mathrm{dBm}$ $P_{\mathrm{Tx,ST}} = -10\,\mathrm{dBm}$, $\mathbb{P}(\mathcal{H}_1) = 1 - \mathbb{P}(\mathcal{H}_0) = 0.2$, $\tau_{\mathrm{est}} = 5\,\mathrm{ms}$, $N_{\mathrm{s}} = 10$ and $N_{\mathrm{p},2} = 1000$.

Firstly, we analyze the performance of the IS in terms of sensing-throughput tradeoff corresponding to the ideal and estimation models by fixing $\tau_{\mathrm{est}} = 5\,\mathrm{ms}$, cf. Fig. 6. In contrast to constraint on $\mathrm{P_d}$ for the ideal model, we employ average and outage constraint for the estimation model. With the inclusion of received power estimation in the frame structure, the ST produces no throughput at the SR for the interval τ_{est}. For the given cases, a suitable sensing time that results in an optimum throughput $\tilde{R}_{\mathrm{s}}(\tau_{\mathrm{est}} = 5\,\mathrm{ms}, \tilde{\tau}_{\mathrm{sen}})$ is determined. Hence, a performance degradation is depicted in terms of the optimum throughput, cf.

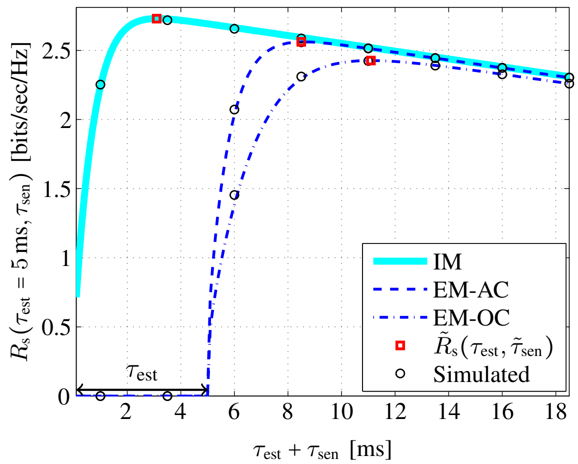

Fig. 6. Sensing-throughput tradeoff for the ideal and estimation models with $\gamma_{p,1} = -10\,dB$ and $\tau_{est} = 5\,ms$.

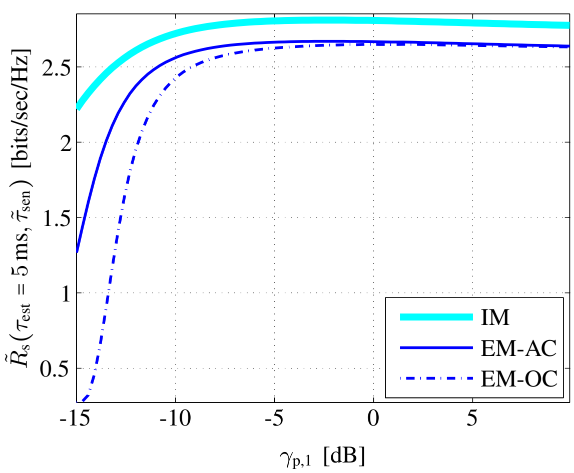

Fig. 7. Optimum throughput versus the $\gamma_{p,1}$ with $\tau_{est} = 5\,ms$.

Fig. 6. For $\kappa = 0.05$, it is observed that the outage constraint is more sensitive to the performance loss in comparison to average constraint. It is clear that the analysis illustrated Fig. 6 is obtained for a certain choice of system parameters, particularly $\gamma_{p,1} = -10\,dB$, $\tau_{est} = 5\,ms$ and $\kappa = 0.05$. To acquire more insights, we consider the effect of variation of these parameters on the performance of IS, subsequently.

Hereafter, for the analysis, we consider the theoretical expressions and choose to operate at suitable sensing time. Next, we determine the variations of the optimum throughput against the received signal to noise ratio $\gamma_{p,1}$ at the ST with $\tau_{est} = 5\,ms$, cf. Fig. 7. For $\gamma_{p,1} < -5\,dB$, the estimation model incurs a significant performance loss. This clearly reveals that the ideal model overestimates the performance of IS. Hence, it is perceived that despite loss in performance, the estimation model is capable of precluding

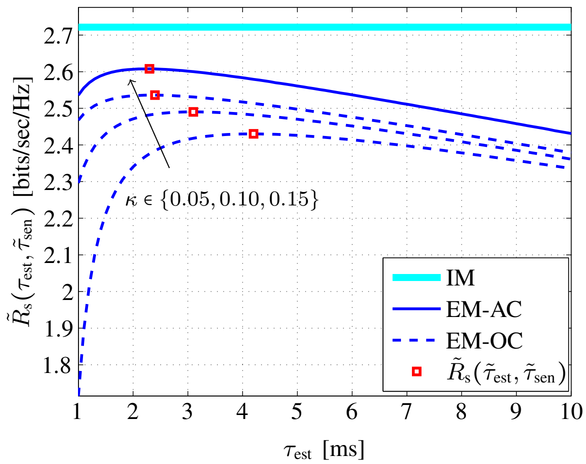

Fig. 8. Estimation-throughput tradeoff for the adjacent and outage constraint with $\gamma_{p,1} = -10\,$dB, where the throughput is maximized over the sensing time. Estimation-throughput tradeoff is utilized to determine a suitable estimation time $\tilde{\tau}_{est}$ that optimizes $\tilde{R}_s$.

interference at the PR, hence, assure reliability to the system.

Upon optimizing the throughput, it is interesting to analyze the variation of optimum throughput against the estimation time. Corresponding to the estimation model, Fig. 8 illustrates a fundamental tradeoff between the estimation time, the sensing time and the throughput. This can be explained from the fact that low values of estimation time results in large variation in P_d. To counteract and satisfy the average and outage constraints, the corresponding thresholds shift to a lower value. This causes an increase in P_{fa}, thereby increasing the sensing-throughput curvature. As a result, the optimum sensing time is obtained at a higher value. However, beyond a certain value ($\tilde{\tau}_{est}$), a further increase in estimation time slightly contributes to performance improvement and largely consumes the time resources. As a consequence to the estimation-sensing-throughput tradeoff, we determine the suitable estimation time that yields an optimum throughput $\tilde{R}_s(\tilde{\tau}_{est}, \tilde{\tau}_{sen})$. Besides that, we consider the variation of optimum throughput for different values of the outage constraint, cf. Fig. 8. It is observed that for the selected the choice of κ, the outage constraint is stringent as compare to the average constraint, hence, results in a lower optimum throughput. Thus, depending on the nature of policy (aggressive or conservative) followed by the regulatory towards interference at the primary system, it is possible to define κ accordingly at the system design.

To procure further insights, we investigate the variations of expected P_d and P_{fa} against the estimation time. From Fig. 9a, it is noticed that the expected P_d corresponding to the outage constraint is strictly

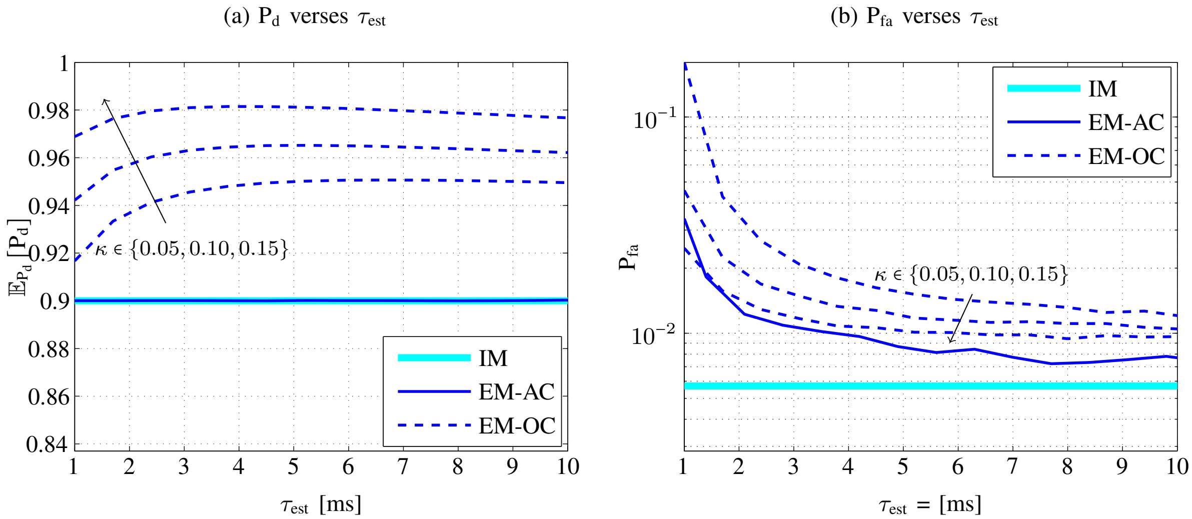

Fig. 9. Variation of $\mathbb{E}_{\mathrm{P_d}}[\mathrm{P_d}]$ and $\mathrm{P_{fa}}$ against the τ_{est}, where the throughput is maximized over the sensing time.

above the desired level $\bar{\mathrm{P}}_{\mathrm{d}}$ for all values of estimation time. For lower value of estimation time, this margin reduces. This is based on the fact that lower estimation time shifts the probability mass of $\mathrm{P_d}$, to lower value, cf. Fig. 3a. Following the previous discussion, it was analyzed that $\mathrm{P_{fa}}$ accounts for a large contribution to the throughput. According to Fig. 9b, $\mathrm{P_{fa}}$ witness a large improvement in performance in the regime $\tau_{\mathrm{est}} \leq 3\,\mathrm{ms}$, however, saturates in the regime $\tau_{\mathrm{est}} \geq 3\,\mathrm{ms}$. Hence, provide further justification to the variation of $\tilde{R}_{\mathrm{s}}(\tau_{\mathrm{est}}, \tilde{\tau}_{\mathrm{sen}})$ against τ_{est} characterized as estimation-sensing-throughput depicted in Fig. 8.

V. Conclusion

In this paper, we have investigated the performance of cognitive radio as interweave system from a deployment perspective. It has been argued that the knowledge of the interacting channels is a key aspect that enables the performance characterization of the IS in terms of sensing-throughput tradeoff. In this regard, a novel model that facilitates the estimation and captures the effect of estimation in the system has been proposed. As a major outcome of the analysis, it has been justified that the existing model, illustrating an ideal scenario, overestimates the performance of the interweave system, hence, unfit for deployment. Moreover, it has been indicated that the distortion induced in the system, specially in the probability of detection may severely degrade the performance of primary system. In order to breakthrough this bottleneck, average and outage constraint as primary user constraints have been proposed. As a consequence, for the estimation model, new expressions of sensing-throughput tradeoff based of the mentioned constraints has been established. Lastly, by analyzing the estimation-sensing-throughput tradeoff, suitable estimation time and sensing time that optimize~~s~~ the throughput at the secondary receiver has been determined.

REFERENCES

[1] A. Kaushik, S. K. Sharma, S. Chatzinotas, B. Ottersten, and F. K. Jondral, "Sensing-Throughput Tradeoff for Cognitive Radio Systems with Unknown Received Power," in *10th International Conference on Cognitive Radio Oriented Wireless Networks and Communications (CROWNCOM)*, April 2015.

[2] J. Andrews *et al.*, "What Will 5G Be?" *IEEE Journal on Selected Areas in Communications*, vol. 32, no. 6, pp. 1065–1082, June 2014.

[3] A. Goldsmith, S. Jafar, I. Maric, and S. Srinivasa, "Breaking Spectrum Gridlock With Cognitive Radios: An Information Theoretic Perspective," *Proceedings of the IEEE*, vol. 97, no. 5, pp. 894–914, May 2009.

[4] E. Axell, G. Leus, E. Larsson, and H. Poor, "Spectrum sensing for cognitive radio : State-of-the-art and recent advances," *IEEE Signal Processing Magazine*, vol. 29, no. 3, pp. 101–116, May 2012.

[5] S. Sharma, S. Chatzinotas, and B. Ottersten, "Exploiting polarization for spectrum sensing in cognitive satcoms," in *CROWNCOM*, June 2012, pp. 36–41.

[6] H. Urkowitz, "Energy detection of unknown deterministic signals," *Proceedings of the IEEE*, vol. 55, no. 4, pp. 523 – 531, april 1967.

[7] V. Kostylev, "Energy detection of a signal with random amplitude," in *ICC*, vol. 3, 2002, pp. 1606–1610 vol.3.

[8] F. Digham, M.-S. Alouini, and M. K. Simon, "On the energy detection of unknown signals over fading channels," in *ICC*, vol. 5, May 2003, pp. 3575–3579.

[9] S. Herath, N. Rajatheva, and C. Tellambura, "Unified approach for energy detection of unknown deterministic signal in cognitive radio over fading channels," in *ICC Workshops*, June 2009, pp. 1–5.

[10] A. Mariani, A. Giorgetti, and M. Chiani, "Energy detector design for cognitive radio applications," in *2010 International Waveform Diversity and Design Conference (WDD)*, Aug 2010, pp. 000 053–000 057.

[11] E. Peh and Y.-C. Liang, "Optimization for cooperative sensing in cognitive radio networks," in *IEEE Wireless Communications and Networking Conference (WCNC)*, March 2007, pp. 27–32.

[12] M. K. Simon and M. S. Alouini, *Digital Communication over Fading Channels: A Unified Approach to Performance Analysis*, 1st ed. New York: Wiley, 2000.

[13] A. Kaushik, M. R. Raza, and F. K. Jondral, "On the Deployment of Cognitive Relay as Underlay Systems," in *CROWNCOM*, Jun. 2014.

[14] Y.-C. Liang, Y. Zeng, E. Peh, and A. T. Hoang, "Sensing-Throughput Tradeoff for Cognitive Radio Networks," *IEEE Transactions on Wireless Communications,*, vol. 7, no. 4, pp. 1326–1337, April 2008.

[15] S. Sharma, S. Chatzinotas, and B. Ottersten, "A hybrid cognitive transceiver architecture: Sensing-throughput tradeoff," in *CROWNCOM*, Jun. 2014.

[16] H. Pradhan, S. Kalamkar, and A. Banerjee, "Sensing-throughput tradeoff in cognitive radio with random arrivals and departures of multiple primary users," *IEEE Communications Letters*, vol. 19, no. 3, pp. 415–418, March 2015.

[17] M. Cardenas-Juarez and M. Ghogho, "Spectrum Sensing and Throughput Trade-off in Cognitive Radio under Outage Constraints over Nakagami Fading," *IEEE Communications Letters*, vol. 15, no. 10, pp. 1110–1113, October 2011.

[18] Y. Sharkasi, M. Ghogho, and D. McLernon, “Sensing-throughput tradeoff for OFDM-based cognitive radio under outage constraints,” in *ISWCS*, Aug 2012, pp. 66–70.

[19] R. Tandra and A. Sahai, “SNR Walls for Signal Detection,” *IEEE Journal of Selected Topics in Signal Processing*, vol. 2, no. 1, pp. 4–17, Feb 2008.

[20] M. Gans, “The effect of gaussian error in maximal ratio combiners,” *IEEE Transactions on Communication Technology*, vol. 19, no. 4, pp. 492–500, August 1971.

[21] W. Gifford, M. Win, and M. Chiani, “Diversity with practical channel estimation,” *IEEE Transactions on Wireless Communications*, vol. 4, no. 4, pp. 1935–1947, July 2005.

[22] ——, “Antenna subset diversity with non-ideal channel estimation,” *IEEE Transactions on Wireless Communications*, vol. 7, no. 5, pp. 1527–1539, May 2008.

[23] R. Annavajjala and L. Milstein, “Performance analysis of linear diversity-combining schemes on rayleigh fading channels with binary signaling and gaussian weighting errors,” *IEEE Transactions on Wireless Communications*, vol. 4, no. 5, pp. 2267–2278, Sept 2005.

[24] H. Suraweera, P. Smith, and M. Shafi, “Capacity limits and performance analysis of cognitive radio with imperfect channel knowledge,” *IEEE Transactions on Vehicular Technology*, vol. 59, no. 4, pp. 1811–1822, May 2010.

[25] H. Kim, H. Wang, S. Lim, and D. Hong, “On the impact of outdated channel information on the capacity of secondary user in spectrum sharing environments,” *IEEE Transactions on Wireless Communications*, vol. 11, no. 1, pp. 284–295, January 2012.

[26] A. Kaushik, S. K. Sharma, S. Chatzinotas, B. Ottersten, and F. K. Jondral, “Estimation-Throughput tradeoff for underlay cognitive radio systems,” *IEEE ICC 2015 - Cognitive Radio and Networks Symposium (ICC’15 (12) CRN)*, Jun. 2015.

[27] A. Kaushik, M. Mueller, and F. K. Jondral, “Cognitive Relay: Detecting Spectrum Holes in a Dynamic Scenario,” in *ISWCS*, Apr. 2013, pp. 1–2.

[28] T. Wang, Y. Chen, E. Hines, and B. Zhao, “Analysis of effect of primary user traffic on spectrum sensing performance,” in *Communications and Networking in China, 2009. ChinaCOM 2009. Fourth International Conference on*, Aug 2009, pp. 1–5.

[29] L. Tang, Y. Chen, E. Hines, and M.-S. Alouini, “Effect of primary user traffic on sensing-throughput tradeoff for cognitive radios,” *IEEE Transactions on Wireless Communications*, vol. 10, no. 4, pp. 1063–1068, April 2011.

[30] B. Zhao, Y. Chen, C. He, and L. Jiang, “Performance analysis of spectrum sensing with multiple primary users,” *IEEE Transactions on Vehicular Technology*, vol. 61, no. 2, pp. 914–918, Feb 2012.

[31] S. Kay, *Fundamentals of Statistical Signal Processing: Detection theory*, ser. Prentice Hall Signal Processing Series. Prentice-Hall PTR, 1998.

[32] I. S. Gradshteyn and I. M. Ryzhik, *Table of Integrals, Series, and Products*, 6th ed. San Diego, CA: Academic Press., 2000.

[33] M. Abramowitz and I. A. Stegun, *Handbook of Mathematical Functions with Formulas, Graphs, and Mathematical Tables*, ninth dover printing, tenth gpo printing ed. New York: Dover, 1964.

[34] F. W. J. Olver, D. W. Lozier, R. F. Boisvert, and C. W. Clark, Eds., *NIST Handbook of Mathematical Functions*. New York, NY: Cambridge University Press, 2010.